

Review

Biomanufacturing human tissues via organ building blocks

Kayla J. Wolf,^{1,4} Jonathan D. Weiss,^{2,4} Sebastien G.M. Uzel,¹ Mark A. Skylar-Scott,^{2,3,*} and Jennifer A. Lewis^{1,*}

¹Wyss Institute for Biologically Inspired Engineering & John A. Paulson School of Engineering and Applied Sciences, Harvard University, 29 Oxford Street, Cambridge, MA 02138, USA

²Department of Bioengineering, Stanford University, 240 Pasteur Drive, Stanford, CA 94304, USA

³BASE Initiative, Betty Irene Moore Children's Heart Center, Lucile Packard Children's Hospital, Stanford University School of Medicine, Stanford, CA 94304, USA

⁴These authors contributed equally

*Correspondence: skyscott@stanford.edu (M.A.S.-S.), jalewis@seas.harvard.edu (J.A.L.)

<https://doi.org/10.1016/j.stem.2022.04.012>

SUMMARY

The construction of human organs on demand remains a tantalizing vision to solve the organ donor shortage. Yet, engineering tissues that recapitulate the cellular and architectural complexity of native organs is a grand challenge. The use of organ building blocks (OBBs) composed of multicellular spheroids, organoids, and assembloids offers an important pathway for creating organ-specific tissues with the desired cellular-to-tissue-level organization. Here, we review the differentiation, maturation, and 3D assembly of OBBs into functional human tissues and, ultimately, organs for therapeutic repair and replacement. We also highlight future challenges and areas of opportunity for this nascent field.

INTRODUCTION

Every day over 150 people join the more than 100,000 patients on the US transplant waitlist and nearly 20 people die as they wait for an available donor organ (<https://organdonor.gov/>). Post transplantation, many recipients will suffer acute rejection within their first year, while chronic rejection and side effects from immunosuppression remain lifelong threats. Moreover, the short viability window of life-saving donor organs limits their deployment to remote locations, resulting in geographical healthcare disparities. The creation of autologous, on-demand organs could overcome these challenges. This vision has been the holy grail of tissue engineering since its inception. However, despite decades of intense research, the biomanufacturing of functional organ-specific tissues remains elusive.

There are myriad difficulties in biomanufacturing human organs, including cell sourcing, vascularization, maturation, attaining physiologic levels of function, developing standards for quality control and safety, and translating to clinical practice. Despite these vast hurdles in *writing* human organs and organ-specific tissues, rapid advances in 3D imaging, genomics, and transcriptomics now allow us to *read* these tissues with unprecedented spatial and temporal detail. Emerging organ-specific and whole-embryo cell atlases offer precise instruction sets for assembling *de novo* tissues (Srivatsan et al., 2021). Yet, paradoxically, the more detail obtained by *reading* organs, the more daunting the task of *writing* them seems. For example, single-cell studies of adult kidneys reveal over 20 different cell types arranged into more than 1 million nephrons per kidney (Park et al., 2018), which are responsible for blood filtration, reabsorption, secretion, and hemostasis (Figure 1). Each nephron contains cells arranged into glomerular and tubular segments with invading and wrapping capillaries that carry out

these critical functions. As another example, closer inspection of the adult human heart has revealed that the traditional delineation of left and right ventricular and atrial cardiomyocytes hides deeper levels of complexity. Using single-cell RNA sequencing, researchers have uncovered the existence of five distinct and spatially localized classes of ventricular cardiomyocytes as well as five classes of atrial cardiomyocytes (Litviňuková et al., 2020). Indeed, *writing de novo* human organs that recapitulate their native counterparts would require the growth, differentiation, maturation, and precise patterning of not just a few, but tens of different cell types.

The grand challenge of organ engineering can therefore be framed as closing the gap between our ability to *read* organs and our ability to *write* them. Fortunately, advances in stem cell generation and differentiation, coupled with advancements in biomanufacturing, are opening new avenues to creating functional human tissues. To generate autologous human organs, one must produce 10–100 billion patient-specific cells, guide their differentiation into distinct and mature phenotypes, pattern these cells into precise 3D architectures, maintain and mature the construct, and surgically implant it. The advent of human induced pluripotent stem cells (hiPSCs), combined with their scalable production and differentiation in suspension culture bioreactors, offers a path to obtaining the necessary raw material (Kropp et al., 2017). Simultaneous innovations that reduce cell media costs are upending the economics of production of human tissues in bulk (Kuo et al., 2020). From a regulatory standpoint, the recent development of genomically engineered hypo-immunogenic hiPSCs can enable the creation of highly characterized and safe universal cell lines to fuel downstream differentiation and biofabrication pipelines (Deuse et al., 2019; Han et al., 2019; Xu et al., 2019). Deriving defined cell types from these pluripotent cells



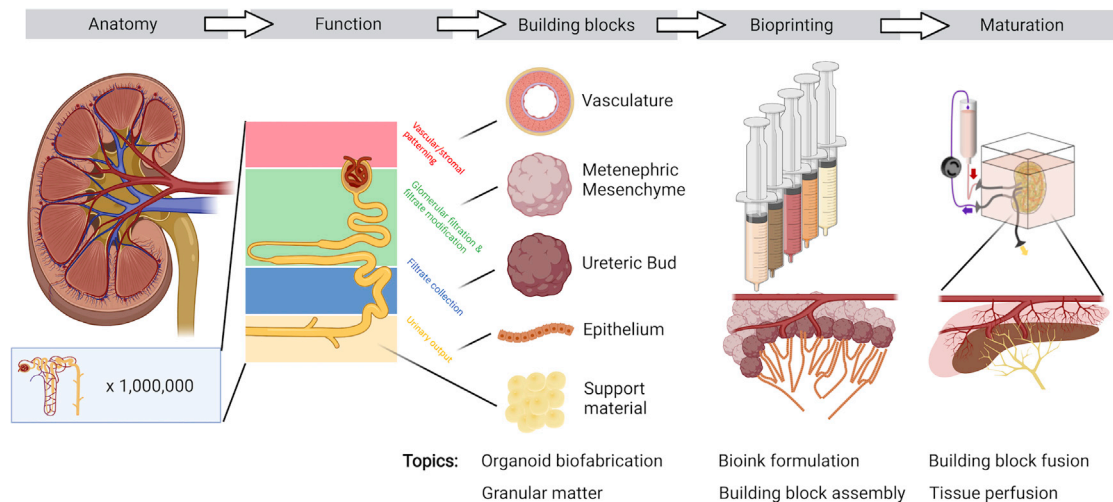


Figure 1. Biomanufacturing human tissues from OBBs

traditionally requires the sequential addition of growth factors or other small molecules; however, emerging efforts are harnessing genomic engineering to deterministically generate targeted cell types of interest. Traditionally, human cells have been seeded onto or into porous scaffolds to produce connective tissues or vascular grafts (Hibino et al., 2011; Kirkton et al., 2019; Niklason et al., 1999). However, this approach lacks the ability to precisely pattern dozens of distinct cell types into organ-specific micro- to macroarchitectures that compose whole human organs.

3D bioprinting enables the programmatic patterning of cell-laden inks and multicellular organ building blocks (OBBs; e.g., embryoid bodies, spheroids, and organoids). All complex solid organs can conceptually be broken down into spatially patterned, or “voxelated,” functional units, each with a distinct cellular and extracellular makeup that bestows homeostatic or physiologic function to the organ. Hence, the roadmap for organ biomanufacturing can be described as a two-step process: (1) render discrete functional units with the requisite cellular components and self-assembled microarchitecture and (2) assemble these functional units into a bulk organ-specific tissue replete with embedded vasculature required to achieve and sustain their function (Figure 1). Within this framework, the key challenges are both maximizing the generation and self-assembly of functional human tissue blocks as well as spatially patterning and maturing these building blocks to produce therapeutic-scale tissues.

Constructing whole organs using single cells as building blocks is currently unfeasible because of inherent scaling limitations of 3D bioprinting (Figure 2). The time required to “pick and place” each cell throughout tissue volumes over 1 mm^3 vastly exceeds the cell viability window ($\sim 1\text{--}2\text{ h}$) during bioprinting. By contrast, the use of multicellular OBBs (e.g., organoids) offers several advantages by both recapitulating the different cell types and microarchitectures within organ-specific tissues as well as vastly reducing the build times required to generate whole organs ($\sim 10^5\text{--}10^6\text{ mm}^3$ in volume) (Miller, 2014). Direct organoid printing is capable of generating human tissues at faster rates because each building block is composed of more than 10^4 cells. However, when patterning tissues at the macroscale, one must simultaneously print the vascular network required to supply

nutrients, clear waste products, and maintain the tissues as they undergo maturation (Kolesky et al., 2014; Miller et al., 2012; Skylar-Scott et al., 2019a). Indeed, embedding vascularization becomes necessary once the fabricated tissue volume exceeds roughly 1 mm^3 , i.e., roughly the size of the individual OBBs. Tissue vascularization can be achieved rapidly using embedded printing methods, such as sacrificial writing into functional tissue (SWIFT) (Skylar-Scott et al., 2019a), wherein a sacrificial ink is printed into a living tissue matrix composed of compacted organoids in the shape of a vascular tree. The subsequent removal of this sacrificial ink leaves behind an interconnected network of cylindrical vessels that can be lined with endothelium, through which nutrients and oxygen can flow.

ORGAN BUILDING BLOCKS

Multicellular aggregates have been used for over a century to study spatial patterning in development (Wilson, 1907), with early studies of mammalian cell aggregates dating to the 1950s (Moscona, 1957). Until recently, multicellular spheroids have been largely generated from primary and immortalized human cells. For example, metabolically active hepatic spheroids have been produced from immortalized lines (Kelm et al., 2003) and primary hepatocytes (Landry et al., 1985). There is emerging interest in assembling these multicellular aggregates into larger tissues. In one of the earliest examples, spheroids were manually placed into rings to form a toroidal tissue architecture within a surrounding 3D matrix (Jakab et al., 2004). This simple yet non-trivial geometry demonstrated the feasibility of generating physiologically relevant forms using multicellular building blocks.

The advent of induced pluripotent stem cells (iPSCs) followed by the development of differentiation protocols that transform these cells into organoids, or “mini-organs,” has radically expanded the functional complexity and types of OBBs that can be generated (Giacomelli et al., 2017; Morizane et al., 2015; Sato et al., 2009; Taguchi et al., 2014; Takasato et al., 2015; Takebe et al., 2013). It is now possible to generate myriad tissue-specific organoids, including cardiac, kidney, liver, and gut spheroids/organoids with exquisite

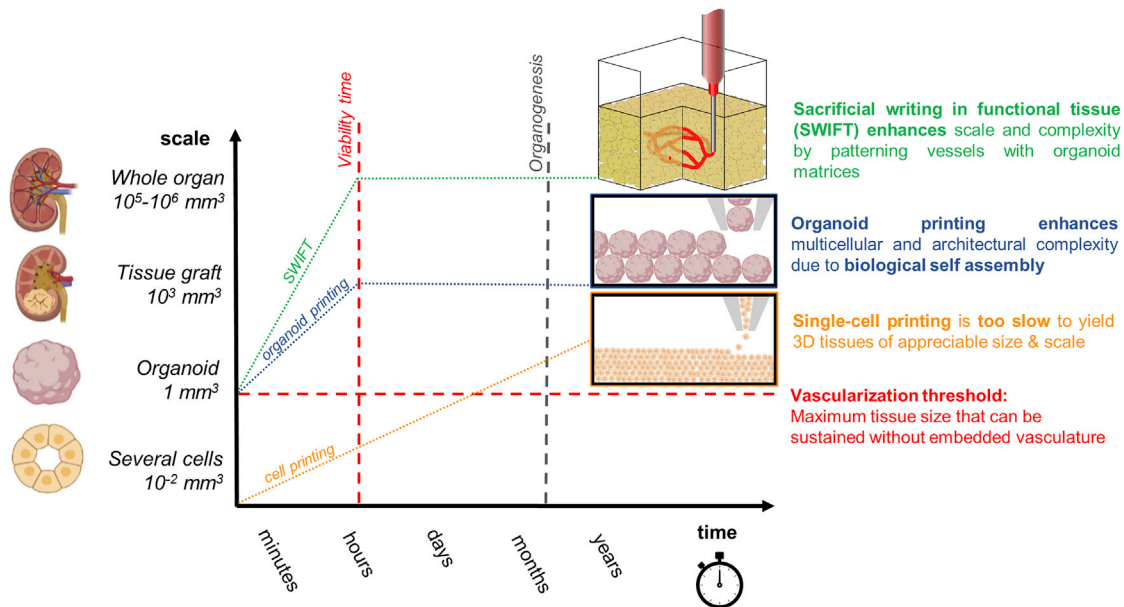


Figure 2. Opportunity space for biomanufacturing human tissues at organ scale

microarchitectures (Figure 3). For example, hiPSC-derived cardiac cells co-cultured with hiPSC-derived endothelial cells yield cardiac spheroids (Giacomelli et al., 2017) that can be further assembled into contractile cardiac tissues that synchronously beat (Breckwoldt et al., 2017). Liver spheroids have also been generated from hiPSCs by combining hiPSC-derived hepatocytes with mesenchymal stem cells and endothelial cells (Takebe et al., 2013). When subjected to perfusion using a microfluidic platform, hepatic aggregates derived from iPSCs have been shown to retain albumin expression for over 28 days (Schepers et al., 2016). To optimize cell-cell interactions, hepatic aggregates have also been patterned from primary hepatocytes, endothelial cells, and stromal cells using a microfabrication method (Stevens et al., 2017). The resulting liver “seeds” can support microstructure formation, including self-organized bile ducts when implanted in animal models. While more advanced liver function will ultimately require an interconnected bile duct network, these seminal studies suggest that liver building blocks may retain structural plasticity that would facilitate functional adaptation *in vivo*. Akin to the liver, kidney organoids require interconnected tubule networks to achieve their ultimate function of filtration and filtrate modification. Several protocols for deriving nephron-rich organoids from metanephric mesenchyme have been recently developed; these organoids possess a cellular composition and structure that resembles a first-trimester kidney (Morizane et al., 2015; Taguchi et al., 2014; Takasato et al., 2014, 2015). However, they generally lack perfusable glomeruli, collecting ducts, and a ureter, hence limiting their functional utility (Little and Combes, 2019; Takasato et al., 2015). Finally, gut organoids (Sato et al., 2009; Spence et al., 2011) have also been generated, and recent work by Brassard et al. has demonstrated that these progenitor cells, when printed into an extracellular matrix (ECM), will spontaneously assemble into an intestinal lumen (Brassard et al., 2020).

Despite the promise of OBBs for biomanufacturing, several hurdles remain. Bulk tissues and organs require a pervasive, hierarchical vascular network to maintain cell viability and function. While bioprinting methods are capable of patterning blood vessels roughly 100 μ m and larger in size, vascularization of individual OBBs at the microscale is needed to fully drive bulk tissue maturation and function. Several strategies, including perfusion, growth factor addition, and matrix cues have been recently reported for inducing microvascularization within spheroids and organoids (Brassard and Lutolf, 2019). For example, Giacomelli et al. enriched iPSC-derived cardiac spheroids with iPSC-derived endothelial cells and demonstrated enhanced expression of cardiac maturation markers, such as genes encoding ion channels and Ca²⁺-handling proteins (Giacomelli et al., 2017). Beyond their role in perfusion, the co-culture of hiPSC-derived cardiomyocytes and cardiac fibroblasts with cardiac endothelial cells has also been shown to improve sarcomeric structure and contractility (Giacomelli et al., 2020). By contrast to direct addition of endothelial cells, physical cues can enhance endothelial cell differentiation and proliferation. Notably, kidney organoids that are subjected to flow during differentiation on an adherent matrix exhibit a 3-fold enrichment in their endothelial progenitor cell population promoting both their vascularization at the microscale and maturation, as observed by significantly enhanced expression of glomerular, tubular, and endothelial markers (Homan et al., 2019).

The complex interplay between microvascular network formation and maturation raises two important questions: (1) what is the optimal differentiation state of OBBs prior to tissue assembly and (2) what is the appropriate balance between spontaneous self-assembly and deterministic biofabrication? At one extreme, a small number of undifferentiated cells could be aggregated and then guided through differentiation, growth, and morphogenesis to form the mature, functional tissue. As a key example of this approach, mouse embryonic stem cell (ESC)-derived cell

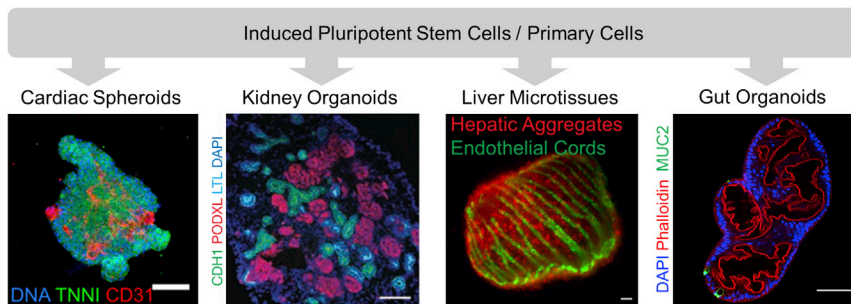


Figure 3. OBBs composed of multicellular spheroids and organoids

Scale bar, left to right: 100, 50, 400, 100 μm . Left to right: images reproduced with permission from Giacomelli et al. (2017); Morizane et al. (2015); Stevens et al. (2017). Far right image was provided courtesy of Joep Beumer, Hubrecht Institute.

aggregates cultured in gastruloid culture conditions and then exposed to cardiogenic factors form cardiovascular progenitors, including first and second heart fields, which undergo morphogenesis resembling the formation of heart chambers (Rossi et al., 2021). Cardiac organoids, exhibiting chamber-like structures, have recently been produced using hiPSCs (Drakhlis et al., 2021; Silva et al., 2021). These strategies recapitulate key features of organogenesis (i.e., spontaneous cell assembly, tissue morphogenesis, and growth) but would require considerable time and resources to reach the scale of whole organs. To circumvent the need for tissue growth, Kupfer et al. deterministically 3D printed immature ESCs into an adult heart shape and then expanded and differentiated the ESCs into cardiovascular phenotypes (Kupfer et al., 2020). The resulting, perfusable heart chambers show continuous action potential propagation with a cardio-effective drug response. At the other extreme, hundreds of thousands of these OBBs can be fully differentiated and deterministically patterned into a large, cohesive cardiac tissue that synchronously beats after several days of maturation (Skylar-Scott et al., 2019a). Because normal tissue morphogenesis is bypassed in this approach, the primary challenge is to ensure adequate OBB fusion via cell-cell and cell-matrix interactions to generate the desired functional output akin to native organs as well as provide sufficient mechanical robustness for handling and suturing during implantation.

BIOPRINTING 3D TISSUES FROM OBBs

Bioprinting organ-specific tissues from multicellular building blocks derived from hiPSCs enables the construction of patient-specific tissues, thereby reducing the risk of immune rejection and enhancing potential for their clinical translation. Several methods have recently emerged for printing tissues from OBBs (Figure 4). Unlike individual cells, spheroid- and organoid-based building blocks are granular in nature, i.e., their characteristic size exceeds roughly 100 μm in diameter, and, hence, their interactions are dominated by gravitational forces. Direct printing of individual spheroids or organoids relies on their granular nature to enable their sequential pick up and placement (Figures 4A and 4B). For example, Ayan et al. showed that different spheroids, including those composed of human umbilical vein endothelial cells (HUVECs), mouse fibroblast cells (3T3), mouse mammary carcinoma cells (4T1), human dermal fibroblasts (HDFs), and human mesenchymal stem cells, could be retrieved from a media bath by aspiration using a glass pipette and then placed onto a matrix-coated substrate (Figure 4A)

in small pyramids and rings. In the presence of HDFs and fibrin, HUVEC-laden spheroids exhibited angiogenic sprouting behavior, which intensified as the distance between adjacent spheroids decreased, likely due to increased cellular signaling.

Expanding upon this approach, Daly et al. and others demonstrated an embedded pick-and-place printing method for creating more complex 3D tissue geometries (Figure 4B) (Ayan et al., 2020b; Daly et al., 2021). This technique relies on similar aspiration pipettes to pick individual spheroids from a media bath and place them within a shear-thinning, self-healing hydrogel support matrix whereupon they remain suspended in 3D space. Using this approach, individual spheroids were used to construct tissue pyramids and layered rings within the hydrogel matrix, from which the tissue could ultimately be harvested (Daly et al., 2021). As one example, spheroids composed of varying mixture ratios of cardiac fibroblasts and iPSC-derived cardiomyocytes were used to create a tissue construct to model post-myocardial infarction scarring. Localized regions rich in cardiac fibroblast spheroids serve as scars that reduce conduction velocity and mechanical contractility compared to control tissues composed solely of cardiomyocyte spheroids. Upon exposing the scarred tissue constructs to Hippo pathway-inhibiting miRNAs for several days, cardiomyocyte proliferation and improved tissue functionality were observed. These examples highlight the ability of pick-and-place methods to produce precisely constructed microtissues for investigating heterogeneous interactions between individual OBBs and for therapeutic drug screening. However, building tissues by patterning OBBs one at a time is slow and thus not well suited for organ-scale bio-manufacturing.

Direct bioprinting of OBB-laden inks offers a higher-throughput method that unlocks therapeutic-scale biofabrication (Figure 4C). Goulart et al. demonstrated the advantage of this method for constructing liver tissues by formulating inks composed of hiPSC-derived hepatic spheroids compared to hepatic cells (Goulart et al., 2020). These inks were printed into toroidal tissue constructs (5 mm high and 10 mm in diameter). After 18 days of culture post printing, the viability and hepatic metabolic function of 3D liver tissue printed from spheroid-laden inks were significantly higher than those produced from cell-laden inks. Thus, the pre-organization of hepatocytes into OBBs with defined microenvironments promoted physiological function at the tissue level. While this method is promising for the scalable generation of organ-scale tissues, two major challenges of direct OBB printing arise once the tissue thickness exceeds a few millimeters. First, as printed tissues become taller, they often lose their shape because of gravity-induced slumping. Second, when the printed tissues exceed

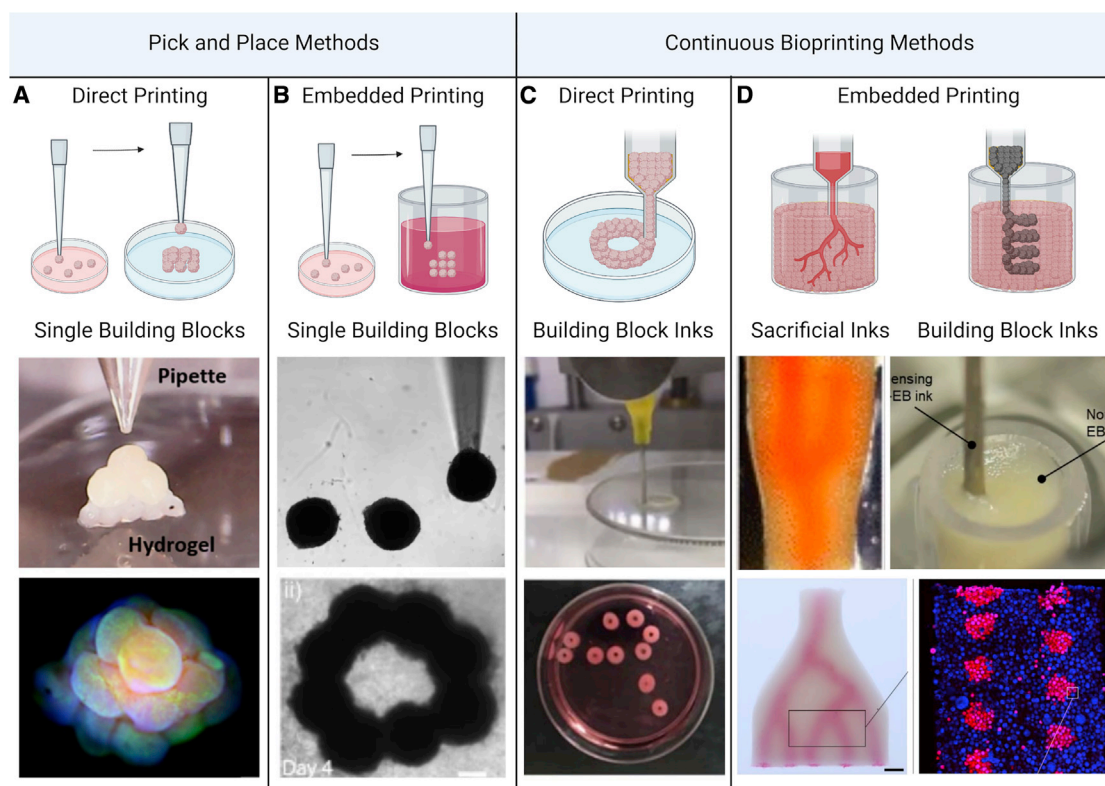


Figure 4. Biomanufacturing of human tissues using OBBs

(A) Direct pick and placement of individual spheroids or organoids.

(B) Embedded pick and placement of individual spheroids or organoids within a support matrix. Scale bar, 200 μm .

(C) Direct printing of spheroid- or organoid-based inks.

(D) Embedded printing of sacrificial inks within a tissue matrix composed of densely packed spheroids or organoids (left) or embedded printing of spheroid- or organoid-based inks in either support (not shown) or tissue (right) matrices. Scale bar, 2 mm.

Images (from left to right) adapted with permission from Ayan et al. (2020a); Daly et al. (2021); Goulart et al. (2020); Skylar-Scott et al. (2019a).

~ 1 mm in thickness, they will undergo necrosis due to a lack of perfusion. While this scale limitation can be addressed by implanting organoids or bioprinted tissues into a host to stimulate neovascularization (Mansour et al., 2018; Takebe et al., 2013), vascular ingrowth is too slow (~ 1 mm/day) to rescue therapeutic-scale tissues.

Embedded 3D printing is an emerging technique that is uniquely capable of printing large-scale tissues replete with vascular networks using soft and biological inks. This method involves printing one viscoelastic ink into another viscoelastic hydrogel or matrix (Wu et al., 2011). The viscoelastic matrix is tailored to be liquid-like enough to enable a printer nozzle to translate through the matrix without tearing it while simultaneously being solid-like enough to adequately support the printed tissue to prevent it from sagging, sinking, or floating. The printed ink can be a sacrificial material that, upon removal, forms a vascular network within a tissue matrix composed of OBBs. Alternatively, the ink can be a cell- or OBB-laden bioink that builds a tissue within a sacrificial or living matrix (Figure 4D). First demonstrated by patterning a sacrificial ink in the form of a hierarchical branching vascular tree within an acellular hydrogel matrix (Wu et al., 2011), this technique has undergone several advances that have enabled the construction of vascularized human tissues at scale. For example, SWIFT allows

complex and branched vascular networks to be embedded within a living tissue matrix composed of OBBs composed of embryoid bodies, organoids, or spheroids derived from hiPSCs (Skylar-Scott et al., 2019a). To attain physiologically relevant scales, these OBBs are cultured in batches of 100,000s, which contain up to half a billion cells. Next, they are mixed with an ECM solution of collagen and Matrigel and compacted into a granular tissue matrix with a total volume of ~ 2.5 mL that contains ~ 200 million cells/mL. A sacrificial gelatin ink is then patterned within the tissue matrix via embedded 3D printing in the form of a vascular network. Upon warming the tissue to 37°C , the sacrificial ink liquifies and can be readily removed from the tissue, leaving behind a perfusable vascular network that sustains the tissue during fusion of the OBBs and subsequent tissue maturation. Using SWIFT, vascularized cardiac tissues were generated and underwent fusion to form a synchronously beating tissue after 1 week of perfusion. With further development, the SWIFT technique could enable biofabrication of vascularized human tissues at organ scale.

Freeform reversible embedding of suspension hydrogels (FRESH) is another important embedded 3D printing technique that enables patterning soft inks at bulk scale with high resolution (Hinton et al., 2015; Lee et al., 2019). This method has been used to create 3D collagen scaffolds in the form of a miniature human

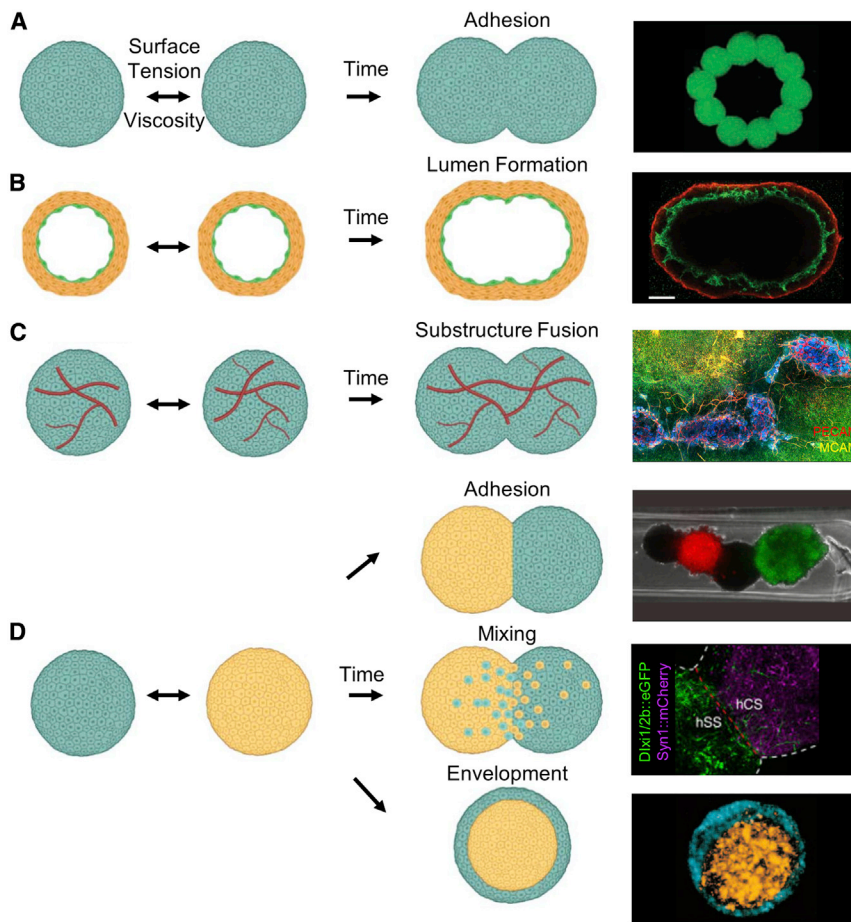


Figure 5. Fusion of spheroid-, organoid-, and assembloid-based OBBs

(A) Homotypic spheroid fusion leading to simple adhesion. Image adapted with permission from Jakab et al. (2004).

(B) Homotypic spheroid fusion of two luminal spheroids generates a spheroid with a single lumen. Image adapted with permission from Fleming et al. (2010). Scale bar, 100 μ m.

(C) Homotypic spheroid fusion with substructure interconnection of vascular networks. Image adapted with permission from Homan et al. (2019).

(D) Heterotypic spheroid fusion leading to simple adhesion, mixing, or envelopment. Scale bar, 200 μ m. Images (top to bottom) adapted with permission from Kim et al. (2018); Birey et al. (2017); Foty et al. (1996).

ventricle model that can be filled with hiPSC-derived cardiomyocytes. Extending this approach, Kupfer et al. demonstrated the feasibility of *in situ* differentiation of printed stem cells after allowing a period of growth and densification (Kupfer et al., 2020). In this case, a bio-ink containing hiPSCs and an ECM composed of methacrylated gelatin (10% or 15%), fibronectin (0–190 μ g/mL), laminin (0–190 μ g/mL), and ColMA (0–5 mg/mL) are printed in a gelatin microparticle support bath via FRESH. The printed structure is based on an MRI scan of a human heart scaled down to the size of a murine heart modified with a single input and output vessel connecting two internal chambers with a wall thickness < 0.5 mm, so vascularization was not required. After 2 weeks in culture to promote hiPSC proliferation, the estimated density of the tissue was \sim 100 million cells/mL, similar to that of native tissue. Cardiac differentiation was then induced post printing, whereupon contiguous electrical function and synchronous beating was observed up to 6 weeks. Looking ahead, co-writing OBBs and vascular networks via embedded 3D printing offers a promising approach for constructing whole organs.

ENHANCING TISSUE FUNCTION VIA BUILDING BLOCK FUSION AND MATURATION

Once assembled into a 3D tissue, OBBs must fuse and form a cohesive network. To date, the fusion of these building blocks

has been primarily explored in simple two-body systems composed of like or unlike spheroids (or organoids) (Figure 5). The viscosity and surface tension of spheroids have been experimentally measured, which suggests that fusion of two spheroids of the same composition is akin to the coalescence of two viscous droplets (Jakab et al., 2010) (Figure 5A). The differential adhesion hypothesis posits that cells will adhere to other like cells provided that all cells remain in a motile state and express similar adhesion molecules. Remarkably, the dynamics of spheroid fusion can, in many cases, be predicted by measuring the physical properties of multicellular aggregates and applying this model

(Jakab et al., 2008; Mironov et al., 2009). For example, spontaneous rounding of tissue fragments, driven by their surface tension, has been observed experimentally (Foty et al., 1996; Jakab et al., 2008), and the time required for fusion has been shown to correlate with cadherin expression (Foty and Steinberg, 2005). However, OBBs are more complex than liquid droplets, so this simple model is not fully predictive. For example, Kosheleva et al. compared the fusion of two mesenchymal spheroids to the fusion of two epithelial spheroids and found that even though the epithelial spheroids had lower surface tension, they underwent faster fusion than their mesenchymal counterparts (Kosheleva et al., 2020).

Many OBBs contain substructures, such as microvascular, tubular, and biliary features, that must ultimately form interconnected networks throughout the biofabricated tissues. Because cells typically adhere most strongly to other like cells, OBBs that contain a mixture of endothelial and supporting cells can spontaneously form lumens. Fleming et al. demonstrated that two hollow spheroids, each containing a vascular lumen surrounded by smooth muscle cells, can fuse to form a single continuous lumen (Fleming et al., 2010). Using this principle, the authors fused multiple spheroids into a single, elongated vessel (Figure 5B). The process of lumen fusion is biologically relevant—for example, the aorta is formed by the fusion of two dorsal aortae (Fleming et al., 2010). While the model implies that

substructure fusion is a secondary phenomenon arising from random movement of differentially adhesive cells, some biological fusion processes are cell directed through chemical gradients, such as vascular anastomosis. Fusion of microvessels between OBBs is necessary to develop a cohesive, perfusable capillary network. While such studies are limited, early examples suggest that vascular fusion is possible. When both microvascularized kidney organoids (Homan et al., 2019) and cardiac spheroids (Polonchuk et al., 2021) fuse together, they appear to form a continuous vasculature network (Figure 5C). Kim et al. also observed fusion of vascular networks between more complex OBBs, i.e., core-shell spheroids (Kim et al., 2019). Interestingly, core-shell spheroids with endothelial cells surrounding stem cells rapidly induced vessel network formation relative to homogeneous spheroids, highlighting the potential for directing tissue fusion through building block design.

The fusion of OBBs may be further complicated or enhanced when they are printed within an ECM, e.g., via FRESH. Interactions between the matrix and embedded spheroids (or organoids) might dictate fusion dynamics. For example, spheroids have been shown to undergo fusion in a collagen matrix with subsequent contraction that depends on the collagen concentration (Jakab et al., 2004). Cell-matrix adhesions may stabilize the shape of spheroids by balancing cell-cell adhesions. For example, vascular spheroids undergoing fusion within a matrix remained ovoid, while they formed spheres absent this matrix (Fleming et al., 2010). Clearly, additional studies that elucidate the competing cell-cell versus cell-matrix interactions that guide the fusion of OBBs within biofabricated human tissues are needed.

The ability to pattern and guide the fusion of different OBBs is important for generating complex tissues. The differential adhesion hypothesis predicts that mismatches in their respective surface tensions would lead to envelopment of the high surface tension spheroid (or organoid) by the lower surface tension counterpart, which has been experimentally observed (Figure 5D) (Foty et al., 1996). However, more complex geometries, known as assembloids, have also been formed by fusing two or more different spheroids (or organoids) together (Jakab et al., 2004; Birey et al., 2017). These assembloids, sometimes in contrast to predictions from the differential adhesion hypothesis, can exist in metastable states and give rise to complex biological interactions. As a simple functional demonstration, Kim et al. fused cardiac myocyte spheroids alternating with cardiac fibroblast spheroids in a line and demonstrated that the cardiac fibroblasts support action potential propagation but with a significant conduction delay (Figure 5D) (Kim et al., 2018). Interestingly, heterotypic fusion of hiPSC-derived dorsal forebrain organoids and ventral forebrain organoids recapitulated *in vivo*-like migration and functional integration of interneurons from the ventral to dorsal region (Figure 5D) (Birey et al., 2017). The differentiation or maturation state of these OBBs can also affect cell behavior and, hence, fusion. Lindberg et al. found that fusion of mesenchymal stromal cell spheroids and articular chondrocyte spheroids, as well as matrix deposition, depends on the timing of contact relative to their maturation state (Lindberg et al., 2021). Hajdu et al. found that their maturation state determines whether spheroids simply adhere or undergo envelopment and that fusion kinetics are related to ECM production

(Hajdu et al., 2010). Collectively, these studies highlight the need for cell-type-dependent fusion studies, especially in heterotypic assemblies.

After assembly, exogenous cues can be provided through embedded vasculature to further promote tissue fusion and maturation. For example, the addition of vascular endothelial growth factor (VEGF) to fusing vascularized cardiac spheroids increased fusion efficiency by more than 2-fold and increased vascular fusion between spheroids (Polonchuk et al., 2021). The construction of human-scale heterogeneous tissues may be seen as a natural extension of assembloids but would require fusion of millions of homotypic and heterotypic spheroids to form patterned tissue. Further work is needed to determine how chemo-mechanical cues, including growth factors, matrix composition, luminal flow, and stretch, support the maturation of spheroids, organoids, assembloids, and, ultimately, biofabricated human organs.

Ultimately, fabricated organ-specific tissues must be functionally integrated with the host tissue; interconnection with the cardiovascular system is critical to perfuse implanted tissues and facilitate tissue function. Small tissue (millimeter scale) constructs might be sufficiently sustained via host-derived microvascular invasion and perfusion, eliminating the need for surgical anastomosis. For example, human iPSC-derived kidney organoids implanted under the renal capsule in mouse were microvascularized by the host after 10–20 days (Sharmin et al., 2016). Interestingly, iPSC-derived glomeruli were preferentially vascularized by the angiogenic host endothelial cells rather than HUVECs co-implanted with the kidney organoids, possibly indicating the importance of vascular flow or HUVEC incompatibility. Human liver seed grafts were also microvascularized by the host after 80 days; grafts contained red blood cells, and microvasculature was formed by both human and mouse endothelial cells, suggesting functional anastomosis (Stevens et al., 2017). However, large tissue grafts will ultimately require hierarchical vasculature with a large vascular inlet and outlet to be surgically anastomosed to the host to facilitate immediate perfusion. In addition, some organs will require additional anastomoses, such as the kidney to the ureter or the liver to the bile duct. Many potential challenges with anastomosis of engineered constructs have been identified or solved through the development of tissue engineered vascular grafts (Kirkton et al., 2019; Patterson et al., 2012). For example, risks include thrombosis, intimal hyperplasia, atherosclerosis, or infection (Pashneh-Tala et al., 2016). Design considerations, such as graft compliance and geometry, at the site of anastomosis could alleviate some potential modes of failure when implanting engineered tissues (Pashneh-Tala et al., 2016).

FUTURE CHALLENGES AND OPPORTUNITIES

Despite the rapid progress, there are several remaining challenges and opportunities for biomanufacturing human tissues and organs at scale. One important hurdle is that the generation of clinical-grade hiPSCs is costly, with estimates of \$1 million per iPSC line (Bravery, 2015). Depending on the differentiation protocol and the size of tissue required, the cost of growth factors and culture supplements are often prohibitive for commercialization (Bravery, 2015). The discovery of low-cost small molecules, such as CHIR-99021, which acts as a Wnt pathway agonist

(Sato et al., 2004), can replace costly growth factors to enable affordable large-scale cultures. Importantly, the fabrication of autologous tissues requires the scalable generation of patient-specific iPSCs, in which each distinct cell line could require modified differentiation protocols to generate the requisite OBBs. This issue could be solved in part by genetic editing of human leukocyte antigens (HLAs) in a standard bank of iPSCs to provide hypo-immunogenic cell lines for broader patient use (Deuse et al., 2019; Han et al., 2019; Xu et al., 2019).

Beyond cost, adapting culture protocols and platforms to be compliant with current good manufacturing practices (cGMP) at scale is another major challenge. Suspension bioreactors are currently the optimal solution for mass cGMP production because of volume efficiency, scalability, and amenability to automated culture, all of which can improve reproducibility (Kropp et al., 2017). However, many hiPSC protocols begin with 2D adherent culture, necessitating either protocol adaptation or the use of less efficient, more costly scaling methods. In addition, many differentiation protocols rely on subjective measures of cell health and differentiation efficiency, such as evaluating confluency and phenotype to determine timing and composition of medium changes (Morizane et al., 2015). Combined with patient-to-patient variability, sex differences, heterogeneity with a single hiPSC line, and genetic drift in subcultures, batch-to-batch reproducibility is a major hurdle (Colter et al., 2021). Biosensors could aid in real-time monitoring of batch quality and control, and a variety of genetic controls, such as microRNA switches, could be applied to purify differentiated cell populations (Miki et al., 2015). In addition to cells, the scalability and manufacturability of any exogenous ECM or scaffolding materials must be considered. Multiple biomaterials have been developed as scaffolds and applied clinically, as thoroughly reviewed elsewhere (Sadtler et al., 2016). In general, synthetic polymers (e.g., polyethylene glycol) offer more control over material properties at a lower cost, while biologically derived materials (e.g., collagen I or fibrin) offer more complex instructive cues critical for some cell culture protocols (Sadtler et al., 2016). Synthetic materials have been modified to incorporate biologically active groups to create scaffolds with tailored mechanical and biological properties. These materials could replace Matrigel in iPSC and organoid culture by mimicking properties such as heparin-like growth factor binding (Aisenbrey and Murphy, 2020). Alternately, patient-specific, biologically derived ECM materials could be obtained directly from the patient, for example, by using omentum tissue derived from a biopsy (Shevach et al., 2015).

Even with the generation of an efficacious therapeutic tissue, safety remains a critical concern. Aside from potential tissue failure, hiPSC tumorigenicity poses a significant risk, which has been demonstrated in animal studies (Lee et al., 2013). Reprogramming of hiPSCs from somatic cells and subsequent subculture compromises genomic integrity, often introducing chromosomal abnormalities in a subpopulation of cells (Hussein et al., 2011). In addition, undifferentiated cells in the engineered tissue could form teratomas (Ben-David and Benvenisty, 2011). There is a growing interest in genetically engineered drug sensitivities or “kill switches” into hiPSC populations as safeguards to eliminate undifferentiated cells on demand (Ando et al., 2015; Martin et al., 2020). In addition, banked hiPSCs that have undergone extensive whole-genomic

analysis could reduce variability and provide a foundation for comparing clinical outcomes (Merkle et al., 2022).

High-throughput, scalable biofabrication methods are needed to fabricate human tissues and, ultimately, whole organs in a practical timescale necessary to maintain cell viability and minimize cost. To date, most extrusion-based bioprinting methods have used printheads composed of one or a few nozzles (Kang et al., 2016; Kolesky et al., 2016). Notably, the build time required to print a full-size human heart composed of 100 μm layers is nearly 100 h using a single 250 μm nozzle (Mirdamadi et al., 2020). Because single nozzles only print one voxel of material at a time, the fabrication time scales roughly with the cube of the tissue volume. Volumetric printing methods can decouple the relationship between printing speed and tissue volume by parallelizing voxel formation. For example, multimaterial, multi-nozzle printheads are capable of simultaneously printing arrays of voxels in a 2D plane, and rapidly switching between bio-inks would facilitate rapid fabrication of intricately patterned tissues (Skylar-Scott et al., 2019b). Light-based bioprinting approaches, such as stereolithography and digital light processing, print layer by layer by applying light to the surface of a photo-reactive resin bed. To date, these methods have been used to rapidly pattern complex, biologically relevant shapes, such as vascular networks at the centimeter scale within an hour (Grigoryan et al., 2019). In computed axial lithography, light is delivered to a liquid resin bed as a series of 2D images at different angles; only regions in which images are superimposed receive enough energy to solidify (Kelly et al., 2019). This approach has been applied to pattern spheroids derived from human liver epithelial organoids into a gel containing a perfusable vascular network (Bernal et al., 2022). However, each of these light-based printing methods requires resins that are compatible with photo-cross-linking, which limits the use of biological matrices and light-sensitive cells. The incorporation of multicellular spheroid, organoid, or assembloid-based OBBs within these photopolymerizable resins will enhance light scattering, limiting the feature resolution and cellular density within the printed tissues. New advances in scalable, high-resolution bioprinting technologies coupled with industrial standardization and cGMP protocols are needed for biomanufacturing clinical-grade human tissues and organs.

A final challenge involves delineating the appropriate balance of OBB maturation before and after tissue biofabrication, which may vary by tissue type. To date, methods for controlling maturation of large-scale human tissues after their assembly have not yet been widely explored. Techniques developed for single organoids or microtissues could be applied to larger tissues as well as bioreactors developed to sustain whole organs prior to transplantation. However, it is unclear whether full maturation *in vitro* is necessary or desirable before implantation. Looking ahead, scientific and technological advances are anticipated across multiple areas—stem cell scale up and differentiation, building block design, fusion, maturation, and biofabrication—and their convergence may soon provide a viable pathway for *de novo* biomanufacturing of organ-specific tissues for therapeutic use.

ACKNOWLEDGMENTS

The authors are grateful for funding provided to the Lewis Lab from ONR Van-
nevar Bush Faculty Fellowship Program (N00014-21-1-2958), Wellcome

Leap's HOPE program, NIDDK (Re)Building a Kidney Consortia (grant# 1UC2DK126023-01), NSF CELL-MET (#EEC-1647837), and the Wyss Institute 3D Organ Engineering Initiative and to the Skylar-Scott Lab from BASE Initiative at Stanford. J.D.W. gratefully acknowledges support from the National Science Foundation Graduate Research Fellowship under grant No. (#DGE-1656518). The authors thank Joep Beumer, Hubrecht Institute, for providing an image of a gut organoid. Figures created with BioRender.com.

AUTHOR CONTRIBUTIONS

J.A.L. and M.A.S.-S. conceived this manuscript. All authors provided input for writing and overall structure of the manuscript. K.J.W., J.D.W., and M.A.S.-S. drafted the manuscript. M.A.S.-S., K.J.W., and J.D.W. generated figures. J.A.L. and M.A.S.-S. edited the manuscript. All authors reviewed and contributed to the final manuscript.

DECLARATION OF INTERESTS

J.A.L. is a cofounder of AcousticaBio and serves as a scientific advisor for Autodesk, Azul3D, Desktop Health (a subsidiary of Desktop Metal), Mooji Meats, and Trestle Biotherapeutics. M.A.S.-S. owns stock in Formlabs, consults for 3D Systems, and is a scientific advisor for AcousticaBio and Mooji Meats. M.A.S.-S., S.G.M.U., and J.A.L. are inventors of the SWIFT biomanufacturing method and have filed a patent on this work. M.A.S.-S. and J.A.L. are inventors on a broader set of patents focused on vascularized human organoids and tissues. Trestle Biotherapeutics has licensed these patents from Harvard University.

REFERENCES

Aisenbrey, E.A., and Murphy, W.L. (2020). Synthetic alternatives to Matrigel. *Nat. Rev. Mater.* 5, 539–551. <https://doi.org/10.1038/s41578-020-0199-8>.

Ando, M., Nishimura, T., Yamazaki, S., Yamaguchi, T., Kawana-Tachikawa, A., Hayama, T., Nakauchi, Y., Ando, J., Ota, Y., Takahashi, S., et al. (2015). A safeguard system for induced pluripotent stem cell-derived rejuvenated T cell therapy. *Stem Cell Rep.* 5, 597–608. <https://doi.org/10.1016/j.stemcr.2015.07.011>.

Ayan, B., Heo, D.N., Zhang, Z., Dey, M., Povilianskas, A., Drapaca, C., and Ozolat, I.T. (2020a). Aspiration-assisted bioprinting for precise positioning of bio-objects. *Sci. Adv.* 6, eaaw5111. <https://doi.org/10.1126/sciadv.aaw5111>.

Ayan, B., Celik, N., Zhang, Z., Zhou, K., Kim, M.H., Banerjee, D., Wu, Y., Costanzo, F., and Ozolat, I.T. (2020b). Aspiration-assisted freeform bioprinting of pre-fabricated tissue spheroids in a yield-stress gel. *Commun. Phys.* 3, 183. <https://doi.org/10.1038/s42005-020-00449-4>.

Ben-David, U., and Benvenisty, N. (2011). The tumorigenicity of human embryonic and induced pluripotent stem cells. *Nat. Rev. Cancer* 11, 268–277. <https://doi.org/10.1038/nrc3034>.

Bernal, P.N., Bouwmeester, M., Madrid-Wolff, J., Falandt, M., Florczak, S., Rodriguez, N.G., Li, Y., Gröbner, G., Samsom, R., Wolferen, M., et al. (2022). Volumetric bioprinting of organoids and optically tuned hydrogels to build liver-like metabolic biofactories. *Adv. Mater.* 34, e2110054.

Birey, F., Andersen, J., Makinson, C.D., Islam, S., Wei, W., Huber, N., Fan, H.C., Metzler, K.R.C., Panagiotakos, G., Thom, N., et al. (2017). Assembly of functionally integrated human forebrain spheroids. *Nature* 545, 54–59. <https://doi.org/10.1038/nature22330>.

Brassard, J.A., and Lutolf, M.P. (2019). Engineering stem cell self-organization to build Better organoids. *Cell Stem Cell* 24, 860–876. <https://doi.org/10.1016/j.stem.2019.05.005>.

Brassard, J.A., Nikolaev, M., Hübscher, T., Hofer, M., and Lutolf, M.P. (2020). Recapitulating macro-scale tissue self-organization through organoid bioprinting. *Nat. Mater.* 20, 22–29. <https://doi.org/10.1038/s41563-020-00803-5>.

Bravery, C.A. (2015). Do human leukocyte antigen-typed cellular therapeutics based on induced pluripotent stem cells make commercial sense? *Stem Cells Dev.* 24, 1–10. <https://doi.org/10.1089/scd.2014.0136>.

Breckwoldt, K., Letuffe-Brenière, D., Mannhardt, I., Schulze, T., Ulmer, B., Werner, T., Benzin, A., Klampe, B., Reinsch, M.C., Laufer, S., et al. (2017). Differentiation of cardiomyocytes and generation of human engineered heart tissue. *Nat. Protoc.* 12, 1177–1197. <https://doi.org/10.1038/nprot.2017.033>.

Colter, J., Murari, K., Biernaskie, J., and Kallos, M.S. (2021). Induced pluripotency in the context of stem cell expansion bioprocess development, optimization, and manufacturing: a roadmap to the clinic. *Npj Regen. Med.* 6, 72. <https://doi.org/10.1038/s41536-021-00183-7>.

Daly, A.C., Davidson, M.D., and Burdick, J.A. (2021). 3D bioprinting of high cell-density heterogeneous tissue models through spheroid fusion within self-healing hydrogels. *Nat. Commun.* 12, 753. <https://doi.org/10.1038/s41467-021-21029-2>.

Deuse, T., Hu, X., Gravina, A., Wang, D., Tediashvili, G., De, C., Thayer, W.O., Wahl, A., Garcia, J.V., Reichenspurner, H., et al. (2019). Hypoimmunogenic derivatives of induced pluripotent stem cells evade immune rejection in fully immunocompetent allogeneic recipients. *Nat. Biotechnol.* 37, 252–258. <https://doi.org/10.1038/s41587-019-0016-3>.

Drakhlis, L., Biswanath, S., Farr, C.M., Lupanow, V., Teske, J., Ritzenhoff, K., Franke, A., Manstein, F., Bolesani, E., Kempf, H., et al. (2021). Human heart-forming organoids recapitulate early heart and foregut development. *Bio-technol.* 39, 737–746. <https://doi.org/10.1038/s41587-021-00815-9>.

Fleming, P.A., Argraves, W.S., Gentile, C., Neagu, A., Forgacs, G., and Drake, C.J. (2010). Fusion of uniluminal vascular spheroids: A model for assembly of blood vessels. *Dev. Dyn.* 239, 398–406. <https://doi.org/10.1002/dvdy.22286>.

Foty, R.A., and Steinberg, M.S. (2005). The differential adhesion hypothesis: a direct evaluation. *Dev. Biol.* 278, 255–263. <https://doi.org/10.1016/j.ydbio.2004.11.012>.

Foty, R.A., Pflieger, C.M., Forgacs, G., and Steinberg, M.S. (1996). Surface tensions of embryonic tissues predict their mutual envelopment behavior. *Development* 122, 1611–1620. <https://doi.org/10.1242/dev.122.5.1611>.

Giacomelli, E., Bellin, M., Sala, L., van Meer, B.J., Tertoolen, L.G.J., Orlova, V.V., and Mummery, C.L. (2017). Three-dimensional cardiac microtissues composed of cardiomyocytes and endothelial cells co-differentiated from human pluripotent stem cells. *Dev.* 144, 1008–1017. <https://doi.org/10.1242/dev.143438>.

Giacomelli, E., Meraviglia, V., Campostri, G., Cochrane, A., Cao, X., van Helden, R.W.J., Krotenberg Garcia, A., Mircea, M., Kostidis, S., Davis, R.P., et al. (2020). Human-iPSC-derived cardiac stromal cells enhance maturation in 3D cardiac microtissues and reveal non-cardiomyocyte contributions to heart disease. *Cell Stem Cell* 26, 862–879.e11. <https://doi.org/10.1016/j.stem.2020.05.004>.

Goulart, E., de Caires-Junior, L.C., Telles-Silva, K.A., Araujo, B.H.S., Rocco, S.A., Sforza, M., de Sousa, I.L., Kobayashi, G.S., Musso, C.M., Assoni, A.F., Oliveira, D., Caldini, E., Raia, S., Lelkes, P.I., and Zatz, M. (2019). 3D bioprinting of liver spheroids derived from human induced pluripotent stem cells sustain liver function and viability in vitro. *Biofabrication* 12, 015010. <https://doi.org/10.1088/1758-5090/ab4a30>.

Grigoryan, B., Paulsen, S.J., Corbett, D.C., Sazer, D.W., Fortin, C.L., Zaita, A.J., Greenfield, P.T., Calafat, N.J., Gounley, J.P., Ta, A.H., et al. (2019). Multi-vascular networks and functional intravascular topologies within biocompatible hydrogels. *Science* 364, 458–464. <https://doi.org/10.1126/science.aav9750>.

Hajdu, Z., Mironov, V., Mehesz, A.N., Norris, R.A., Markwald, R.R., and Viscconti, R.P. (2010). Tissue spheroid fusion-based in vitro screening assays for analysis of tissue maturation. *J. Tissue Eng. Regenerative Med.* 4, 659–664. <https://doi.org/10.1002/term.291>.

Han, X., Wang, M., Duan, S., Franco, P.J., Kenty, J.H.R., Hedrick, P., Xia, Y., Allen, A., Ferreira, L.M.R., Strominger, J.L., et al. (2019). Generation of hypoimmunogenic human pluripotent stem cells. *Proc. Natl. Acad. Sci. U. S. A.* 116, 10441–10446. <https://doi.org/10.1073/pnas.1902566116>.

Hibino, N., Villalona, G., Pietris, N., Duncan, D.R., Schoffner, A., Roh, J.D., Yi, T., Dobrucki, L.W., Mejias, D., Sawh-Martinez, R., et al. (2011). Tissue-engineered vascular grafts form neovessels that arise from regeneration of the adjacent blood vessel. *FASEB J.* 25, 2731–2739. <https://doi.org/10.1096/fj.11-182246>.

Hinton, T.J., Jallerat, Q., Palchesko, R.N., Park, J.H., Grodzicki, M.S., Shue, H.J., Ramadan, M.H., Hudson, A.R., and Feinberg, A.W. (2015). Three-dimensional printing of complex biological structures by freeform reversible embedding of suspended hydrogels. *Sci. Adv.* 1, e1570075. <https://doi.org/10.1126/sciadv.1500758>.

- Homan, K.A., Gupta, N., Kroll, K.T., Kolesky, D.B., Skylar-Scott, M., Miyoshi, T., Mau, D., Valerius, M.T., Ferrante, T., Bonventre, J.V., et al. (2019). Flow-enhanced vascularization and maturation of kidney organoids in vitro. *Nat. Methods* 16, 255–262. <https://doi.org/10.1038/s41592-019-0325-y>.
- Hussein, S.M., Batada, N.N., Vuoristo, S., Ching, R.W., Autio, R., Närvä, E., Ng, S., Sourour, M., Härmäläinen, R., Olsson, C., et al. (2011). Copy number variation and selection during reprogramming to pluripotency. *Nature* 471, 58–62. <https://doi.org/10.1038/nature09871>.
- Jakab, K., Neagu, A., Mironov, V., Markwald, R.R., and Forgacs, G. (2004). Engineering biological structures of prescribed shape using self-assembling multicellular systems. *Proc. Natl. Acad. Sci. U. S. A.* 101, 2864–2869. <https://doi.org/10.1073/pnas.0400164101>.
- Jakab, K., Damon, B., Marga, F., Doaga, O., Mironov, V., Kosztin, I., Markwald, R., and Forgacs, G. (2008). Relating cell and tissue mechanics: Implications and applications. *Dev. Dyn.* 237, 2438–2449. <https://doi.org/10.1002/dvdy.21684>.
- Jakab, K., Norotte, C., Marga, F., Murphy, K., Vunjak-Novakovic, G., and Forgacs, G. (2010). Tissue engineering by self-assembly and bio-printing of living cells. *Biofabrication* 2, 022001. <https://doi.org/10.1088/1758-5082/2/2/022001>.
- Kang, H.W., Lee, S.J., Ko, I.K., Kengla, C., Yoo, J.J., and Atala, A. (2016). A 3D bioprinting system to produce human-scale tissue constructs with structural integrity. *Nat. Biotechnol.* 34, 312–319. <https://doi.org/10.1038/nbt.3413>.
- Kelly, B.E., Bhattacharya, I., Heidari, H., Shusteff, M., Spadaccini, C.M., and Taylor, H.K. (2019). Volumetric additive manufacturing via tomographic reconstruction. *Science* 363, 1075–1079. <https://doi.org/10.1126/science.aau7114>.
- Kelm, J.M., Timmins, N.E., Brown, C.J., Fussenegeger, M., and Nielsen, L.K. (2003). Method for generation of homogeneous multicellular tumor spheroids applicable to a wide variety of cell types. *Biotechnol. Bioeng.* 83, 173–180. <https://doi.org/10.1002/bit.10655>.
- Kim, E.M., Lee, Y., Bin, Kim, S., Jeong, Park, J., Lee, J., Kim, S.W., Park, H., and Shin, H. (2019). Fabrication of core-shell spheroids as building blocks for engineering 3D complex vascularized tissue. *Acta Biomater.* 100, 158–172. <https://doi.org/10.1016/j.actbio.2019.09.028>.
- Kim, T.Y., Kofron, C.M., King, M.E., Markes, A.R., Okundaye, A.O., Qu, Z., Mende, U., and Choi, B.R. (2018). Directed fusion of cardiac spheroids into larger heterocellular microtissues enables investigation of cardiac action potential propagation via cardiac fibroblasts. *PLoS One* 13, e0196714. <https://doi.org/10.1371/journal.pone.0196714>.
- Kirkton, R.D., Santiago-Maysonet, M., Lawson, J.H., Tente, W.E., Dahl, S.L.M., Niklason, L.E., and Prichard, H.L. (2019). Bioengineered human acellular vessels recellularize and evolve into living blood vessels after human implantation. *Sci. Transl. Med.* 11, 1–12. <https://doi.org/10.1126/scitranslmed.aau6934>.
- Kolesky, D.B., Truby, R.L., Gladman, A.S., Busbee, T.A., Homan, K.A., and Lewis, J.A. (2014). 3D bioprinting of vascularized, heterogeneous cell-laden tissue constructs. *Adv. Mater.* 26, 3124–3130. <https://doi.org/10.1002/adma.201305506>.
- Kolesky, D.B., Homan, K.A., Skylar-Scott, M.A., and Lewis, J.A. (2016). Three-dimensional bioprinting of thick vascularized tissues. *Proc. Natl. Acad. Sci.* 113, 3179–3184. <https://doi.org/10.1073/pnas.1521342113>.
- Kosheleva, N.V., Efremov, Y.M., Shavkuta, B.S., Zurina, I.M., Zhang, D., Zhang, Y., Minaev, N.V., Gorkun, A.A., Wei, S., Shpichka, A.I., et al. (2020). Cell spheroid fusion: Beyond liquid drops model. *Sci. Rep.* 10, 12614–12615. <https://doi.org/10.1038/s41598-020-69540-8>.
- Kropp, C., Massai, D., and Zweigert, R. (2017). Progress and challenges in large-scale expansion of human pluripotent stem cells. *Process. Biochem.* 59, 244–254. <https://doi.org/10.1016/j.procbio.2016.09.032>.
- Kuo, H.H., Gao, X., DeKeyser, J.M., Fetterman, K.A., Pinheiro, E.A., Weddle, C.J., Fonoudi, H., Orman, M.V., Romero-Tejeda, M., Jouni, M., et al. (2020). Negligible-cost and weekend-free chemically defined human iPSC culture. *Stem Cell Rep.* 14, 256–270. <https://doi.org/10.1016/j.stemcr.2019.12.007>.
- Kupfer, M.E., Lin, W.H., Ravikumar, V., Qiu, K., Wang, L., Gao, L., Bhuiyan, D.B., Lenz, M., Ai, J., Mahutga, R.R., et al. (2020). In situ expansion, differentiation, and electromechanical coupling of human cardiac muscle in a 3D bio-printed, chambered organoid. *Circ. Res.* 127, 207–224. <https://doi.org/10.1161/circresaha.119.316155>.
- Landry, J., Bernier, D., Ouellet, C., Goyette, R., and Marceau, N. (1985). Spheroidal aggregate culture of rat liver cells: Histotypic reorganization, biomatrix deposition, and maintenance of functional activities. *J. Cell Biol.* 101, 914–923. <https://doi.org/10.1083/jcb.101.3.914>.
- Lee, A., Hudson, A.R., Shiwardski, D.J., Tashman, J.W., Hinton, T.J., Yemini, S., Bliley, J.M., Campbell, P.G., and Feinberg, A.W. (2019). 3D bioprinting of collagen to rebuild components of the human heart. *Science* 365, 482–487. <https://doi.org/10.1126/science.aav9051>.
- Lee, A.S., Tang, C., Rao, M.S., Weissman, I.L., and Wu, J.C. (2013). Tumorigenicity as a clinical hurdle for pluripotent stem cell therapies. *Nat. Med.* 19, 998–1004. <https://doi.org/10.1038/nm.3267>.
- Lindberg, G.C.J., Cui, X., Durham, M., Veenendaal, L., Schon, B.S., Hooper, G.J., Lim, K.S., and Woodfield, T.B.F. (2021). Probing multicellular tissue fusion of cocultured spheroids—a 3D-bioassembly model. *Adv. Sci.* 8, 2103320. <https://doi.org/10.1002/advsc.202103320>.
- Little, M.H., and Combes, A.N. (2019). Kidney organoids: Accurate models or fortunate accidents. *Genes Dev.* 33, 1319–1345. <https://doi.org/10.1101/gad.329573.119>.
- Litvinuková, M., Talavera-López, C., Maatz, H., Reichart, D., Worth, C.L., Lindberg, E.L., Kanda, M., Polanski, K., Heinig, M., Lee, M., et al. (2020). Cells of the adult human heart. *Nature* 588, 466–472. <https://doi.org/10.1038/s41586-020-2797-4>.
- Mansour, A.A., Gonçalves, J.T., Bloyd, C.W., Li, H., Fernandes, S., Quang, D., Johnston, S., Parylak, S.L., Jin, X., and Gage, F.H. (2018). An in vivo model of functional and vascularized human brain organoids. *Nat. Biotechnol.* 36, 432–441. <https://doi.org/10.1038/nbt.4127>.
- Martin, R.M., Fowler, J.L., Cromer, M.K., Lesch, B.J., Ponce, E., Uchida, N., Nishimura, T., Porteus, M.H., and Loh, K.M. (2020). Improving the safety of human pluripotent stem cell therapies using genome-edited orthogonal safeguards. *Nat. Commun.* 11, 2713. <https://doi.org/10.1038/s41467-020-16455-7>.
- Merkle, F.T., Ghosh, S., Genovese, G., Handsaker, R.E., Kashin, S., Meyer, D., Karczewski, K.J., O'Dushlaine, C., Pato, C., Pato, M., et al. (2022). Whole-genome analysis of human embryonic stem cells enables rational line selection based on genetic variation. *Cell Stem Cell* 29, 472–486.e7. <https://doi.org/10.1016/j.stem.2022.01.011>.
- Miki, K., Endo, K., Takahashi, S., Funakoshi, S., Takei, I., Katayama, S., Toyoda, T., Kotaka, M., Takaki, T., Umeda, M., et al. (2015). Efficient Detection and Purification of cell populations using synthetic MicroRNA switches. *Cell Stem Cell* 16, 699–711. <https://doi.org/10.1016/j.stem.2015.04.005>.
- Miller, J.S. (2014). The billion cell construct: will three-dimensional printing get us there? *Plos Biol.* 12, e1001882–9. <https://doi.org/10.1371/journal.pbio.1001882>.
- Miller, J.S., Stevens, K.R., Yang, M.T., Baker, B.M., Nguyen, D.-H.T., Cohen, D.M., Toro, E., Chen, A.A., Galie, P.A., Yu, X., et al. (2012). Rapid casting of patterned vascular networks for perfusable engineered three-dimensional tissues. *Nat. Mater.* 11, 768–774. <https://doi.org/10.1038/nmat3357>.
- Mirdamadi, E., Tashman, J.W., Shiwardski, D.J., Palchesko, R.N., and Feinberg, A.W. (2020). FRESH 3D bioprinting a full-size model of the human heart. *ACS Biomater. Sci. Eng.* 6, 6453–6459. <https://doi.org/10.1021/acsbomaterials.0c01133>.
- Mironov, V., Visconti, R.P., Kasyanov, V., Forgacs, G., Drake, C.J., and Markwald, R.R. (2009). Organ printing: tissue spheroids as building blocks. *Biomaterials* 30, 2164–2174. <https://doi.org/10.1016/j.biomaterials.2008.12.084>.
- Morizane, R., Lam, A.Q., Freedman, B.S., Kishi, S., Valerius, M.T., and Bonventre, J.V. (2015). Nephron organoids derived from human pluripotent stem cells model kidney development and injury. *Nat. Biotechnol.* 33, 1193–1200. <https://doi.org/10.1038/nbt.3392>.
- Moscona, A. (1957). The development in vitro of chimeric aggregates of dissociated embryonic chick and mouse cells. *Proc. Natl. Acad. Sci.* 43, 184–194. <https://doi.org/10.1073/pnas.43.1.184>.
- Niklason, L.E., Gao, J., Abbott, W.M., Hirschi, K.K., Houser, S., Marini, R., and Langer, R. (1999). Functional arteries grown in vitro. *Science* 284, 489–493. <https://doi.org/10.1126/science.284.5413.489>.

- Park, J., Shrestha, R., Qiu, C., Kondo, A., Huang, S., Werth, M., Li, M., Barasch, J., and Suszták, K. (2018). Single-cell transcriptomics of the mouse kidney reveals potential cellular targets of kidney disease. *Science* 360, 758–763. <https://doi.org/10.1126/science.aar2131>.
- Pashneh-Tala, S., MacNeil, S., and Claeysens, F. (2016). The tissue-engineered vascular graft - Past, present, and future. *Tissue Eng. - Part B Rev.* 22, 68–100. <https://doi.org/10.1089/ten.teb.2015.0100>.
- Patterson, J.T., Gilliland, T., Maxfield, M.W., Church, S., Naito, Y., Shinoka, T., and Breuer, C.K. (2012). Tissue-engineered vascular grafts for use in the treatment of congenital heart disease: from the bench to the clinic and back again. *Regen. Med.* 7, 409–419. <https://doi.org/10.2217/rme.12.12>.
- Polonchuk, L., Surija, L., Lee, M.H., Sharma, P., Liu Chung Ming, C., Richter, F., Ben-Sefer, E., Rad, M.A., Mahmodi Sheikh Sarmast, H., Shamery, W.A., et al. (2021). Towards engineering heart tissues from bioprinted cardiac spheroids. *Biofabrication* 13, 045009. <https://doi.org/10.1088/1758-5090/ac14ca>.
- Rossi, G., Broguiere, N., Miyamoto, M., Boni, A., Guiet, R., Girgin, M., Kelly, R.G., Kwon, C., and Lutoff, M.P. (2021). Capturing cardiogenesis in gastruloids. *Cell Stem Cell* 28, 230–240.e6. <https://doi.org/10.1016/j.stem.2020.10.013>.
- Sadtler, K., Singh, A., Wolf, M.T., Wang, X., Pardoll, D.M., and Elisseeff, J.H. (2016). Design, clinical translation and immunological response of biomaterials in regenerative medicine. *Nat. Rev. Mater.* 1, 16040. <https://doi.org/10.1038/natrevmats.2016.40>.
- Sato, N., Meijer, L., Skaltsounis, L., Greengard, P., and Brivanlou, A.H. (2004). Maintenance of pluripotency in human and mouse embryonic stem cells through activation of Wnt signaling by a pharmacological GSK-3-specific inhibitor. *Nat. Med.* 10, 55–63. <https://doi.org/10.1038/nm979>.
- Sato, T., Vries, R.G., Snippert, H.J., Van De Wetering, M., Barker, N., Stange, D.E., Van Es, J.H., Abo, A., Kujala, P., Peters, P.J., and Clevers, H. (2009). Single Lgr5 stem cells build crypt-villus structures in vitro without a mesenchymal niche. *Nature* 459, 262–265. <https://doi.org/10.1038/nature07935>.
- Schepers, A., Li, C., Chhabra, A., Seney, B.T., and Bhatia, S. (2016). Engineering a perfusable 3D human liver platform from iPS cells. *Physiol. Behav.* 16, 2644–2653. <https://doi.org/10.1039/c6lc00598e>.
- Sharmin, S., Taguchi, A., Kaku, Y., Yoshimura, Y., Ohmori, T., Sakuma, T., Mukoyama, M., Yamamoto, T., Kurihara, H., and Nishinakamura, R. (2016). Human induced pluripotent stem cell-derived podocytes mature into vascularized glomeruli upon experimental transplantation. *J. Am. Soc. Nephrol.* 27, 1778–1791. <https://doi.org/10.1681/asn.2015010096>.
- Shevach, M., Zax, R., Abrahamov, A., Fleischer, S., Shapira, A., and Dvir, T. (2015). Omentum ECM-based hydrogel as a platform for cardiac cell delivery. *Biomed. Mater.* 10, 034106. <https://doi.org/10.1088/1748-6041/10/3/034106>.
- Silva, A.C., Matthys, O.B., Joy, D.A., Kauss, M.A., Natarajan, V., Lai, M.H., Turaga, D., Blair, A.P., Alexanian, M., Bruneau, B.G., and McDevitt, T.C. (2021). Co-emergence of cardiac and gut tissues promotes cardiomyocyte maturation within human iPSC-derived organoids. *Cell Stem Cell* 28, 2137–2152.e6. <https://doi.org/10.1016/j.stem.2021.11.007>.
- Skylar-Scott, M.A., Uzel, S.G.M., Nam, L.L., Ahrens, J.H., Truby, R.L., Damaraju, S., and Lewis, J.A. (2019a). Biomanufacturing of organ-specific tissues with high cellular density and embedded vascular channels. *Sci. Adv.* 5, eaaw2459. <https://doi.org/10.1126/sciadv.aaw2459>.
- Skylar-Scott, M.A., Mueller, J., Visser, C.W., and Lewis, J.A. (2019b). Voxellated soft matter via multimaterial multinozzle 3D printing. *Nature* 575, 330–335. <https://doi.org/10.1038/s41586-019-1736-8>.
- Spence, J.R., Mayhew, C.N., Rankin, S.A., Kuhar, M.F., Vallance, J.E., Tolle, K., Hoskins, E.E., Kalinichenko, V.V., Wells, S.I., Zorn, A.M., et al. (2011). Directed differentiation of human pluripotent stem cells into intestinal tissue in vitro. *Nature* 470, 105–109. <https://doi.org/10.1038/nature09691>.
- Srivatsan, S.R., Regier, M.C., Barkan, E., Franks, J.M., Packer, J.S., Grosjean, P., Duran, M., Saxton, S., Ladd, J.J., Spielmann, M., et al. (2021). Embryoscale, single-cell spatial transcriptomics. *Science* 373, 111–117. <https://doi.org/10.1126/science.abb9536>.
- Stevens, K.R., Scull, M.A., Ramanan, V., Fortin, C.L., Chaturvedi, R.R., Knouse, K.A., Xiao, J.W., Fung, C., Mirabella, T., Chen, A.X., et al. (2017). In situ expansion of engineered human liver tissue in a mouse model of chronic liver disease. *Sci. Transl. Med.* 9, 5505. <https://doi.org/10.1126/scitranslmed.aah5505>.
- Taguchi, A., Kaku, Y., Ohmori, T., Sharmin, S., Ogawa, M., Sasaki, H., and Nishinakamura, R. (2014). Redefining the in vivo origin of metanephric nephron progenitors enables generation of complex kidney structures from pluripotent stem cells. *Cell Stem Cell* 14, 53–67. <https://doi.org/10.1016/j.stem.2013.11.010>.
- Takasato, M., Er, P.X., Becroft, M., Vanslambrouck, J.M., Stanley, E.G., Elfant, A.G., and Little, M.H. (2014). Directing human embryonic stem cell differentiation towards a renal lineage generates a self-organizing kidney. *Nat. Cell Biol.* 16, 118–126. <https://doi.org/10.1038/ncb2894>.
- Takasato, M., Er, P.X., Chiu, H.S., Maier, B., Baillie, G.J., Ferguson, C., Parton, R.G., Wolvetang, E.J., Roost, M.S., Chuva de Sousa Lopes, S.M., and Little, M.H. (2015). Kidney organoids from human IPS cells contain multiple lineages and model human nephrogenesis. *Nature* 526, 564–568. <https://doi.org/10.1038/nature15695>.
- Takebe, T., Sekine, K., Enomura, M., Koike, H., Kimura, M., Ogaeri, T., Zhang, R.-R., Ueno, Y., Zheng, Y.-W., Koike, N., et al. (2013). Vascularized and functional human liver from an iPSC-derived organ bud transplant. *Nature* 499, 481–484. <https://doi.org/10.1038/nature12271>.
- Wilson, H.V. (1907). On some phenomena of coalescence and regeneration in sponges. *J. Elisha Mitchell Sci. Soc.* 5, 245–258. <https://doi.org/10.1002/jez.1400050204>.
- Wu, W., Deconinck, A., and Lewis, J.A. (2011). Omnidirectional printing of 3D microvascular networks. *Adv. Mater.* 23, H178–H183. <https://doi.org/10.1002/adma.201004625>.
- Xu, H., Wang, B., Ono, M., Kagita, A., Fujii, K., Sasakawa, N., Ueda, T., Gee, P., Nishikawa, M., Nomura, M., et al. (2019). Targeted disruption of HLA genes via CRISPR-Cas9 generates iPSCs with enhanced immune compatibility. *Cell Stem Cell* 24, 566–578.e7. <https://doi.org/10.1016/j.stem.2019.02.005>.